Commercial microwave links for urban drainage modelling: The effect of link characteristics and their position on runoff simulations

Jaroslav PASTOREK*[a], Martin FENCL[a], Jörg RIECKERMANN[b], Vojtěch BAREŠ[a]

[a] Department of Hydraulics and Hydrology, Czech Technical University in Prague, Thákurova 7, 166 29 Prague 6, Czech Republic
[b] Department Urban Water Management, Eawag, Überlandstrasse 133, CH-8600 Dübendorf, Switzerland

*Corresponding author: jaroslav.pastorek@fsv.cvut.cz
Other authors: martin.fencl@cvut.cz; joerg.rieckermann@eawag.ch; vojtech.bares@cvut.cz

Abstract

Rainfall observations are crucial when designing and operating urban drainage systems. However, rainfall data of sufficient quality for urban drainage modelling are often unavailable. Commercial microwave links (CMLs), radio connections widely used in telecommunication networks, can provide path-integrated quantitative precipitation estimates (QPEs) which could conveniently complement traditional precipitation observations. We investigate the suitability of individual CMLs to provide relevant QPEs for rainfall-runoff simulations. We are interested especially in CML characteristics influencing the accuracy of rainfall measurements, and in the effect of the CML position (in relation to the catchment) on the spatial representativeness of the measurements. We work with a 3-year long experimental data set from a small (1.3 km^2) urban catchment located in Prague, Czech Republic. We use QPEs from real-world CMLs as inputs for urban rainfall-runoff modelling and we assess the modelling performance by comparing the simulated runoffs with observed stormwater discharges. The results show that the model performance is related both to the CML sensitivity to rainfall and to the CML position. The bias propagated into the runoff predictions is proportional to the CML path length, with the largest errors for the shortest CMLs. The effect of the CML position is especially pronounced during heavy rainfalls, when QPEs from shorter CMLs located within or close-to catchment borders reproduce runoff dynamics better than QPEs from CMLs reaching far outside of the catchment. Adjusting CML QPEs to remote rain gauges substantially reduces their bias. However, the adjusting worsens the ability of the CML QPEs to reproduce runoff dynamics during heavy rainfalls.

Key words

commercial microwave links; opportunistic sensing; rainfall-runoff modelling; rainfall monitoring; urban catchment;

1 Introduction

Urban drainage systems are designed to drain both the foul sewage from households or industry and the stormwater from land surfaces in urban areas, using combined or separate sewer networks. However, excessive amounts of stormwater loading the drainage systems, typically during storm events, often lead to undesired effects such as urban pluvial flooding (Zevenbergen et al., 2008), health risk due to pathogenic organisms (ten Veldhuis et al., 2010), decreased treatment efficiency of wastewater treatment plants (Rauch and Harremoes, 1996), or substantial hydraulic stress to aquatic biota of receiving waters accompanied by negative impacts on water quality (Ellis, 2000). Therefore, operational management of the quantity and quality of urban stormwater runoff is a serious concern in urban environmental management (Tsihrintzis and Hamid, 1997).

Since precipitation is the essential driver of runoff processes in urban areas, rainfall observations are the key input data when designing and operating urban drainage systems during wet weather periods. Nowadays, mitigation of negative effects of urban drainage on the society and the environment is often related to methods and concepts which require operational rainfall products with high spatial and/or temporal resolution (Einfalt et al., 2004) . Such rainfall observations are employed in real time control (RTC) strategies to optimize treatment processes at WWTP (Schuetze et al., 2004) or to minimize impacts of sewer overflows (Vezzaro and Grum, 2014). Furthermore, these data are used for extreme event analysis, e.g. for evaluation of insurance damage claims (Spekkers et al., 2013) or for operational warnings (Montesarchio et al., 2009). The importance of operational rainfall data is increased by ongoing climate changes (van der Pol et al., 2015), which are expected to increase the intensity and frequency of heavy rainfalls in many areas around the world (Willems et al., 2012).

Current rainfall monitoring practices

The availability of rainfall data of sufficient quality is inadequate for the most of the Earth's land surface. Furthermore, the coverage by surface precipitation gauging networks is worsening in many regions around the world (Lorenz and Kunstmann, 2012). Global precipitation data sets can be obtained from satellite missions, but the accuracy and spatiotemporal resolution of these observations is still not sufficient for usage in hydrological modelling of small mountainous or urban catchments (Kidd and Huffman, 2011).

The requirements on temporal and spatial resolution of rainfall data are higher in urban catchments (e.g. Schilling, 1991; Berne et al., 2004) because they differ from natural ones in several aspects from the hydrological point of view. Firstly, scales of areas examined in urban and natural catchment hydrology typically differ in orders of magnitude. Secondly, urban areas are covered by a high ratio of impermeable surfaces, what not only limits rainfall infiltration, but as well leads to more surface runoff (e.g. causing higher peak flows) and higher dynamics of the runoff process (e.g. faster runoff concentration).

Tipping bucket rain gauges represent the traditional way of retrieving precipitation measurements in urban areas. However, these devices often fail to provide sufficient information about the spatiotemporal variability of rainfall, typically due to low densities of rain gauge networks. Especially when heavy storm events, which are crucial for evaluation of urban stormwater systems, are considered, the spatial representativeness of point rainfall observations from rain gauges is limited (Emmanuel et al., 2012).

Weather radar observations have been extensively studied in recent years. Due to limitations inherent to this technology (indirect rainfall measurement, often in relatively high altitudes above the ground and far away from the radar), radar rainfall data are typically, in order to be useful for hydrological modelling, adjusted to rainfall measurements from rain gauges (Harrison et al., 2009). These adjustments usually reduce mean areal bias of rainfall fields, but, as well, often destroy small scale spatial structure of local extremes (Wang et al., 2015). However, neglecting rainfall spatiotemporal variability at small scales can lead to substantial errors in runoff modelling of urban catchments (e.g. Gires et al., 2012). The smoothing of local extremes could be reduced by adjusting to dense rain gauge networks. Nevertheless, it has been concluded that traditionally available rain gauge networks and adjustment techniques do not meet the high requirements of urban hydrology (Wang et al., 2013; Borup et al., 2016). Although the usage of weather radars for urban water management applications has been extensively researched in recent years and a substantial progress has been made towards reliable high quality data, many challenges still remain unsolved. For example, it is difficult to quantify uncertainty arising from the discrepancy between the catch area of a rain gauge (order of 10^{-2} m^2) and the area of a radar pixel (order of 10^4-10^6 m^2) (e.g. Anagnostou et al., 1999). Similarly, adjusting radar data in operational mode is both a methodological and a technical challenge because rain gauge data are often delivered with delay. Finally, the availability of weather radars is mostly limited to developed countries (Heistermann et al., 2013), and even in these regions, there are observational gaps where radar observations are not available in a desired spatiotemporal resolution.

Opportunistic precipitation data collection

Opportunistic precipitation sensing can provide rainfall data from new types of devices, which could conveniently complement traditional precipitation observation networks, and thus improve rainfall data availability. Recent development of various financially accessible hardware and software solutions has made the measurement with purpose-made sensors widely available throughout many different fields (Swan, 2012). Inexpensive purpose-made sensors are becoming more common as well among experimental hydrologists (e.g. Tauro et al., 2018). Furthermore, there are numerous online amateur weather networks that aggregate and visualize citizen-contributed weather observations (Gharesifard et al., 2017). One of such platforms (Weather Underground) collects data from more than 250,000 mainly personal weather stations (de Vos et al., 2017). Data gathered in this way could, therefore, notably enhance the density of in-situ precipitation observation. However, quality control of such crowdsourced data (and associated metadata) from amateur weather stations is very challenging, since these devices are often not calibrated or regularly maintained. Furthermore, similarly as for radar rainfall observations, this kind of data has been so far available chiefly only in developed regions. Therefore, for developing countries, where the scarcity of precipitation monitoring networks is a more pressing issue, the relevancy of crowdsourced precipitation data is still very limited.

Apart from crowdsourcing or low-cost sensors in general, the opportunistic sensing of precipitation can be performed as well by taking advantage of other devices. Instead of the direct observation of precipitation, certain devices get distorted by it, and from this distortion, the information about the rainfall can be extracted, like in the case of commercial microwave links.

Commercial microwave links

Commercial microwave links (CMLs) are point-to-point radio connections widely used as cellular backhaul. A substantial part of CML networks is operated at frequencies between 20 - 40 GHz, where radio wave attenuation caused by raindrops is almost proportional to rainfall intensity. These CMLs can be, therefore, used as unintentional rainfall sensors providing path-integrated quantitative precipitation estimates (QPEs). Moreover, CML data are accessible online in real time from network operation centers either through network monitoring systems or through specifically designed server sided applications (Chwala et al., 2016).

Deriving precipitation estimates from the attenuation of microwaves was originally suggested several decades ago (Atlas and Ulbrich, 1977). This idea has experienced a renaissance in recent years, probably thanks to the extensive growth of GSM networks (Messer et al., 2006, Leijnse et al., 2007), which often incorporate CMLs. Recently, there has been about four million CMLs being used worldwide within cellular networks and this number is still increasing (Ericsson, 2016).

CMLs represent a promising supplement to traditional measurements from ground rain gauges and radars. They can contribute to improving water resources management, especially in areas where traditional infrastructure for rainfall measurement is in generally insufficient (Gosset et al., 2016). Since CML networks are typically very dense in urbanized areas, CML QPEs could be especially convenient for urban drainage modelling, an application where rainfall information of high spatiotemporal resolution is required.

The relationship between the raindrop-induced attenuation A_r [dB] and rainfall intensity R [mm/h] is robust and well understood. For a given rainfall intensity, A_r is proportional to CML length and frequency. The relation can be expressed using the following approximation:

$$(1)\ R = \alpha\ (A_r / L)^{\beta},$$

where L [m] is the length of a given CML, and α [mm/h km$^{\beta}$ dB$^{-\beta}$] and β [-] are empirical parameters depending on CML frequency and polarization, and on drop size distribution (Olsen et al., 1978).

Nonetheless, A_r must be separated from other components of total (observed) attenuation A [dB], for which purpose the following relation is often used:

$$(2)\ A_r = (A - A_w - B),$$

where A_w [dB] stands for the attenuation caused by antenna wetting, and B [dB] for rainfall-independent “baseline” attenuation. The latter can be identified from dry-weather attenuation levels. However, A_w is difficult to quantify because antenna wetting is a complex process influenced, besides rainfall, also by other atmospheric conditions such as wind, temperature, humidity or solar radiation, but also by antenna radome material or coating (Leth et al., 2018). This complexity (and site-specificity) is probably the reason why wet antenna attenuation models suggested in the literature are often based on different assumptions. For example, Kharadly and Ross (2001) assumes A_w being dependent on rainfall intensity and suggests to estimate it by an exponential relation to the total measured attenuation. Leijnse et al. (2008) attempted to describe A_w by a physically based model relating A_w to the thickness of the water film on the antenna surface, which is assumed to be power-law related to rainfall intensity. Overeem et al. (2011)

proposed pragmatic approach assuming constant A_w over the whole observation period, where A_w is assumed to be the same for all CMLs operating at a given frequency band. Schleiss et al. (2013) suggested that A_w is not correlated to rainfall intensity but increases after the rain has started with gradual antenna wetting up to a predefined saturation point, and then again decreases after the rain has stopped. Reported drying times are up to six hours. This illustrates that A_w quantification is still challenging.

The magnitude of A_w is, unlike the magnitude of raindrop-induced attenuation A_r, independent of CML length. Results of previous studies suggest that A_w is also relatively insensitive to CML frequency at bands used for CML rainfall estimation. Thus, QPEs from CMLs less sensitive to raindrop-induced attenuation A_r, i.e. CMLs with shorter paths and lower frequencies, are prone to be relatively more affected by A_w than CMLs more sensitive to the A_r. For example, for a CML 1 km long and working at the frequency of 32 GHz, the attenuation caused by a rainfall of 20 mm/h is about 4 dB. However, for a CML with the same frequency and path length of 4 km, A_r equals roughly 15 dB. If we overestimate A_r derived from the measured total attenuation A by 1 dB, what is a common value due to the uncertainties associated to the quantification of A_w, then the derived precipitation rate will be overestimated by approximately 30% for the 1-km CML, and by 10% for the 4-km one (see Fig. 1). Nevertheless, if the rainfall intensity is only 3 mm/h, the relative errors in CML QPEs rise to 175% and 40%, for the 1-km and 4-km CMLs respectively. Moreover, for low precipitation rates, the CML frequency becomes an important factor as well, with higher errors associated to lower frequencies.

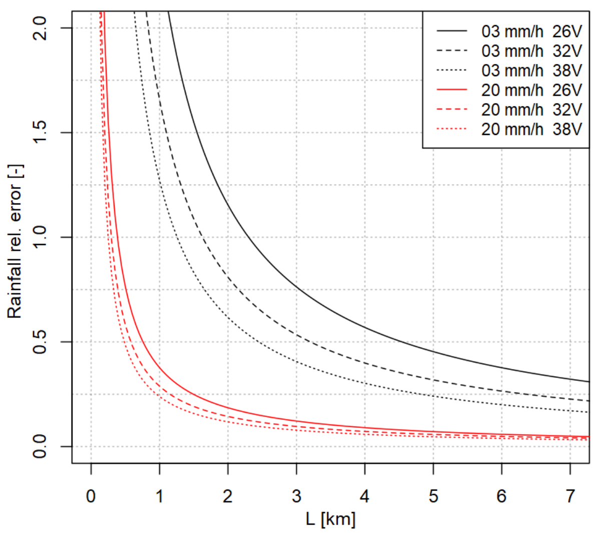

Fig. 1. The relative error in QPEs from CMLs with vertical polarization for two rainfall intensities (3 and 20 mm/h) and three CML frequencies (26, 32, 38 GHz), as caused by an error of 1 dB in the estimate of wet antenna attenuation.

Moreover, quantization of the records of transmitted and received radio signal power, which are used to calculate the total observed attenuation, can have a similar effect as the imprecise estimation of the attenuation due to wet antenna. Commonly used quantization levels, such as 1 dB for the transmitted and 0.33 dB for the received signal power, make from CMLs relatively insensitive (and thus not very precise) rainfall sensors.

Interestingly, short CMLs are potentially the most informative for urban drainage modeling, since their path lengths typically correspond well to spatial scales of urban subcatchments. This might not be true if we tried to reconstruct spatially distributed rainfall, e.g. by means of linear tomography (Giuli et al., 1991; D'Amico et al., 2016), or later proposed non-linear tomography (Zinevich et al., 2008). However, CML networks are not ideal grids but they have rather star-shaped topologies. Thus, tomographic reconstruction would not enable to reconstruct small-scale variability using only long CMLs.

In order to reduce the systematic errors in CML QPEs, Fencl et al. (2017) proposed a novel method for adjusting QPEs from CMLs to measurements from traditional rain gauges. According to Fencl et al. (2017), this approach can provide precise high-resolution precipitation estimates, even if the rain gauges used for adjusting are remote from the catchment in order of kilometers and provide data with temporal aggregation of up to one hour.

However, it is not clear how errors in CML QPEs propagate through hydrological models, how correction methods designed to reduce the bias, e.g. by adjusting to rain gauge observations, influence modelling outputs, or what are the characteristics that make a CML suitable to be used as a source of QPEs for urban drainage modelling. Moreover, it is as well unclear how to use these unintentional opportunistic rainfall sensors for standard hydrological and engineering tasks. For example, it is unknown whether CML QPEs are, due to existing infrastructure and low additional operational costs, best suited for operational usage in urban drainage modelling, or whether they can be conveniently used as well for model calibration. Similarly, it remains unclear whether they can be used alone or rather in combination with traditional rainfall measurement devices.

In fact, there has not been much research on the effect of CML QPEs on hydrological predictions. Smiatek et al. (2017) investigated the potential of QPEs from CMLs for streamflow prediction and water balance analyses in an orographically complex mountainous region. In the field of urban drainage modelling, there is a study of Stránský et al. (2018), where it is concluded that CML QPEs (adjusted to traditional rain gauge data using the method suggested by Fencl et al., 2017) can outperform rain gauges used alone when reproducing runoff dynamics. However, the study was performed in a single urban catchment and with a relatively limited amount of rainfall observations (11 rainfall-runoff events), thus it could not address in detail factors which influence the performance of CMLs as rainfall sensors and, as well, could not draw conclusions on appropriate selection of CMLs suitable for rainfall-runoff modeling.

Objectives of the study

Our study aims on improving the understanding of the potential part of CML QPEs in urban drainage modelling. More specifically, we address the ability of CMLs of various characteristics and positions within the studied catchment to provide relevant rainfall data for urban rainfall-runoff modelling.

This is done by utilizing QPEs from a real-world CML network as inputs for an urban rainfall-runoff model. We evaluate the model performance for CML QPEs from various observation layouts and we compare it with the model performance obtained using rain gauge data from permanent municipal observation network. The performance criteria are evaluated by comparing the simulated runoffs with observed stormwater discharges. We do this while employing an extensive data set which was being collected during three summer seasons and which contains data from 19 CMLs located in a wider area of the studied urban catchment.

2 Material and methods

Experimental catchment

The experimental urban catchment (Fig. 2) with the area of 1.3 km^2 lies in Prague-Letňany, Czech Republic, and it is drained by a separate stormwater sewer system. Approximately 35% of the catchment area is covered by impervious surfaces. The catchment is slightly inclined to the north, with the altitude gradually declining from roughly 280 to 250 m above the sea level. The lag time between rainfall peak and runoff peak observed at the outlet from the catchment is approximately 20 minutes.

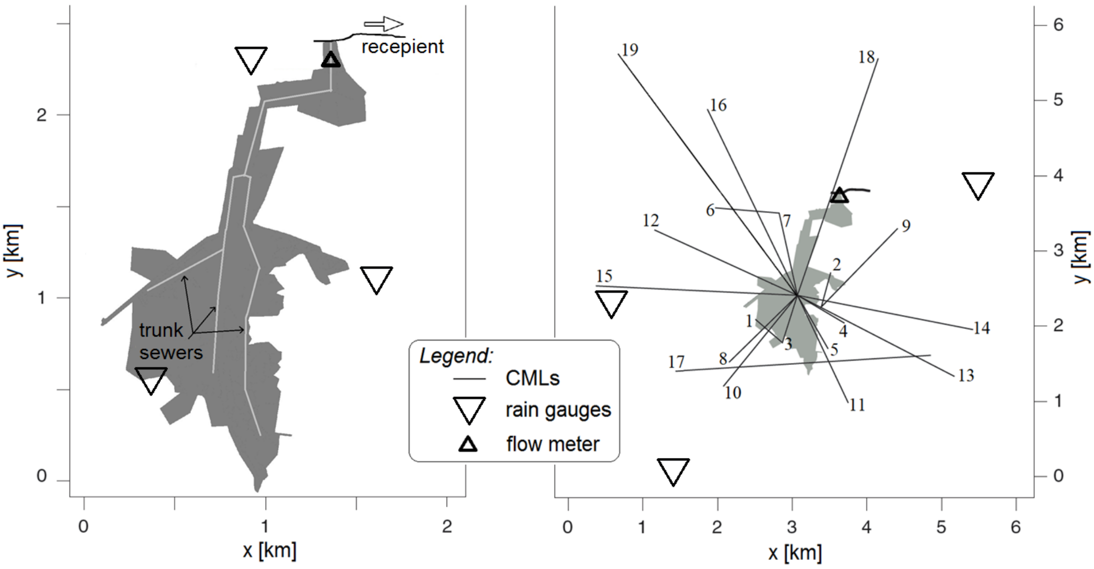

Fig. 2: Left: Schematic layout of the studied urban catchment and the rain gauges used for model calibration. Right: Location of the CMLs (with IDs denoted) and of the municipal rain gauges. The CML central node is located close to the catchment centroid. Longer CMLs reach out of the catchment by several kilometers.

Data retrieval

We monitored 19 CMLs (Tab. 1) located in the catchment and its surroundings (Fig. 2) for a period between July 2014 and October 2016, excluding the winter months. The CMLs broadcast at 25 to 39 GHz frequencies, their lengths are between 611 and 5795 m, and they are operated by a major telecommunication service provider. Data from CMLs were retrieved at 10-s resolution (for details, see Fencl et al., 2015) and aggregated to 1-min resolution.

Moreover, observations from three tipping bucket rain gauges operated by the municipal sewer authority, each in a distance of approximately 2.5 km from the catchment (Fig. 2, right), were collected at 1-min resolution during the same period. The rain gauges were manufactured by the Meteoservis company (MR3 model) and they are regularly maintained and dynamically calibrated (Humphrey et al., 1997). They have the funnel area of 500 cm^2, the bucket volume of 5 ml, and their single tip corresponds to approximately 0.1 mm of rainfall.

ID	FreqA [GHz]	FreqB [GHz]	Polarization	Length [m]
1	31.82	32.63	V	611
2	32.63	NA	H	645
3	NA	32.63	V	816
4	38.88	38.6	V	911
5	24.55	25.56	V	1022
6	37.62	37.62	V	1086
7	37.62	38.88	V	1396
8	37.62	38.88	V	1584
9	31.82	32.63	V	1858
10	24.55	25.56	H	1953
11	38.88	NA	V	1979
12	31.82	32.63	V	2611
13	24.55	25.56	V	2957
14	24.55	25.56	V	3000
15	24.55	25.56	V	3195
16	24.55	25.56	V	3432
17	25.56	24.55	V	4253
18	24.55	25.56	V	4523
19	24.55	25.56	V	5795

Tab. 1: Characteristics of CMLs. FreqA and FreqB are CML frequencies for both directions. The NA value indicates that records in respective directions are not available. Polarization (Vertical/Horizontal) is the same for both directions.

In addition, we measured discharges at the stormwater drainage system outlet using an area-velocity flow meter (Triton, ADS). Temporal resolution of the discharge measurements is 2 min for wet and 10 min for dry periods. Observed discharge values range approximately from 2 to 2000 l/s. Following the Guide to the expression of uncertainty in measurement (International Bureau of Weights and Measures and International Organization for Standardization, 1993), we have estimated the standard uncertainty and the expanded uncertainty of the measured flow rate. Input variables used to derive the flow rate, i.e. pipe radius R [m], measured flow depth h [m] and measured cross sectional velocity U [m.s^{-1}] are assumed uncorrelated. The following values of input variables are propagated to estimate the standard uncertainty: the pipe radius R = 0.75 m, the standard uncertainty in the pipe radius $u(R)$ = 0.0015 m, and the flow depth h = [0.15; 0.375; 0.75] m corresponding to [10; 25; 50]% of pipe filling. This range of flow depths corresponds to observations in the sewer cross section during the selected rainfall events. Since the flow regime of interest is unsteady turbulent flow during storm events, we follow the suggestion of Muste et al. (2012) and we assume the standard uncertainty of measured flow depth as $u(h)$ = 0.015 m. Finally, the velocity in cross section is assumed to be U = [0.99; 1.73; 2.47] m.s^{-1} for the given flow depths, and its standard uncertainty is estimated as $u(U) = 0.05U$. The expanded uncertainty of measured discharge $U(Q) = ku_c(Q)$ based on a t-distribution (at 95 % level of confidence) with k = 2 gives $U(Q)$ = [0.0282; 0.090; 0.245] m^3.s^{-1}, equivalent to ± [31.0%; 15%; 11%] of the total value Q = [0.091; 0.590; 2.17] m^3.s^{-1}.

Deriving CML QPEs

Several steps are necessary to estimate the precipitation-induced attenuation for a given CML and to derive the associated precipitation rates. First, total radio wave attenuation is calculated for each of the two CML channels as the difference between the transmitted and received signal level. Second, a quality check is performed to identify CML erratic behavior which has to be filtered out.

The following behavior is regarded as erratic: i) sudden peaks where, within two time steps, the signal level increases and then decreases (or reversely) by more than 5 dB, ii) longer periods (days) with no signal fluctuation, and iii) periods with random noise larger than 2 dB. Third, attenuation data are aggregated to regular 1-min time series by averaging attenuation values within 1-min intervals. Fourth, attenuation time series from the both CML channels are averaged. Fifth, baseline attenuation is estimated with a low-pass filter parameter m = 0.00145 (according to Fenicia et al., 2012).

After the baseline separation, we proceed in deriving CML QPEs in the two different ways: i) by using the model described by the Eq. 1 and Eq. 2 with parameters taken from literature, and ii) by a simplified linear attenuation-rainfall model adjusted to rain gauges (according to Fencl et al., 2017). In the first approach, we apply wet antenna correction (A_w from Eq. 2) as a constant offset in accordance with Overeem et al. (2011). Parameters α and β from Eq. 1 are chosen as recommended by ITU Radiocommunication Sector (2005). In the second method, the mean of the instantaneous values of the three municipal rain gauges (Fig. 2, right), aggregated to 15-min time steps, is used for adjusting the wet antenna attenuation A_w and the parameter α, while keeping β equal to one, as proposed by Fencl et al. (2017).

Rainfall-runoff model

To simulate the discharges at the drainage system outlet, we use an EPA-SWMM model calibrated using an independent dataset, i.e. measurements obtained before the experimental period of this study from three rain gauges only temporarily installed in the catchment (Fig. 2, left). The rainfall-runoff model was built using detailed information about the catchment (e.g. ratio of impervious areas for individual subcatchments) and the drainage system (e.g. pipe materials and diameters) kindly provided by the municipal water management authority.

The reliability of model prediction was tested using rainfall data from three rain gauges only temporarily installed in the catchment, i.e. the same devices that were used for the model calibration. This verification was performed for a dataset obtained in the same period as the rainfall data from CMLs we subsequently analyze in the study, i.e. between July 2014 and October 2016. Results of this verification are summarized for all relevant rainfall-runoff events from this period in Tab. 2. These results suggest that the model reproduces runoff well with the relative error in volume on average only 1.9 % and with strong correlation to observed values (Pearson's correlation coefficient PCC = 0.95). Slightly worse performance in terms of Nash–Sutcliffe efficiency (mean and stand. deviation equal to 0.73 and 0.41) is mainly caused by model deficiency when reproducing peak flows during heavy rainfalls. The simulated maximal discharges are in these situations often substantially overestimated (in average by 50%). For some of the heaviest rainfalls, the peak flows are overestimated by up to 100%, probably because such events have not been used when calibrating the model.

	dV [-]	NSE [-]	PCC [-]
Mean	0.019	0.734	0.952
Standard deviation	0.175	0.411	0.052

Tab. 2: Results of the rainfall-runoff model verification as evaluated by the relative error of the total runoff volume (dV), the Nash–Sutcliffe efficiency (NSE), and the Pearson correlation coefficient (PCC).

Modelling scenarios and performance evaluation

We use CML QPEs (derived in the two above described ways) as inputs into the (above described) calibrated rainfall-runoff model, and we simulate discharges at the drainage system outlet. Overall, we use rainfall data from 41 different observation layouts as precipitation inputs into the model, thus we study 41 scenarios. The rainfall inputs are always implemented as areal precipitation in the model, i.e. the rainfall intensity is assumed not to vary above the studied catchment.

Firstly, we employ QPEs derived from only one CML at a time, consecutively using each of the 19 CMLs. Next, we construct a time series calculated as the mean over all available CML QPEs for every time step. Thus, we construct 20 time series for each of the two methods of deriving CML QPEs. Additionally, in order that we can compare CML QPEs with a traditional way of rainfall monitoring, the mean of the three rain gauges from the permanent municipal network is used as model input. These are the same rain gauges as those used for CML adjusting, but we use the original 1-min resolution in this case.

The rainfall-runoff simulations are not performed continuously for the whole observation period, but only for individual rainfall-runoff events causing relevant discharges (rainfall depth over 2 mm). The model performance is evaluated, for the 41 studied scenarios and each of the simulated events, by comparing the simulated runoffs and observed stormwater discharges. Nash–Sutcliffe efficiency (NSE, [-]), the Pearson correlation coefficient (PCC, [-]), and the relative error of the total runoff volume (dV, [-]) are used as modelling performance metrics.

Data availability

During the monitoring period (July 2014 - October 2016), we observed 105 relevant rainfalls with total depth exceeding 2 mm. However, due to outages in rain gauge, flow meter, and CML observations, we were able to perform simulations only for 71 of these events. Furthermore, we have excluded from the evaluation rainfall events with less than two thirds of CMLs available (events 1-9, 23, 32, and 42) and three CMLs (#1, #2, #10) which experience long outages during the experimental period. The evaluation is, therefore, performed for 16 CMLs and 59 events. The overall availability of CML data is shown in Fig. 3.

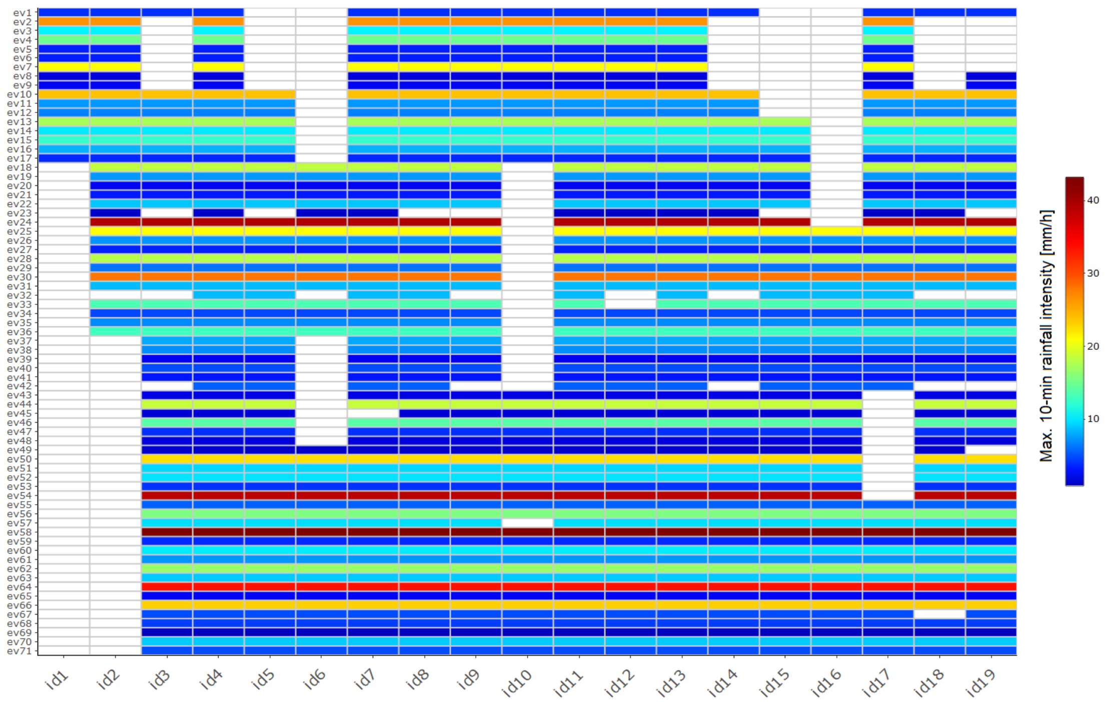

Fig. 3: Availability of the rainfall data for the 19 CMLs during 71 rainfall events with color-coded maximal 10-min rainfall intensities.

3 Results

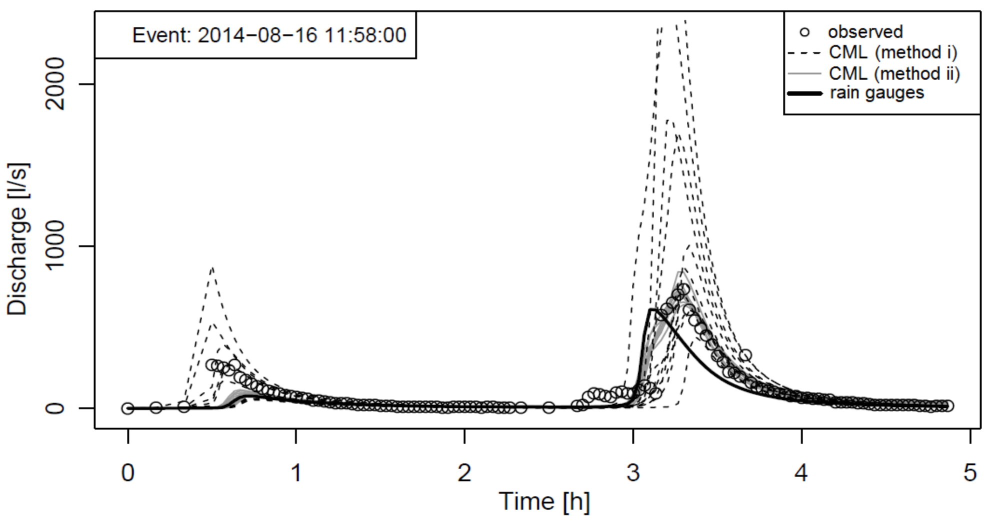

Fig. 4: Modelled and observed discharges for a selected rainfall-runoff event. The values obtained using the unadjusted CML QPEs (method i) reach up to 3800 l/s.

Firstly, we present results obtained for a single rainfall-runoff event (Fig. 4) which illustrates well the potential of using CML QPEs for urban drainage modelling. Discharges modelled using the CML QPEs adjusted to rain gauges (method ii) fit the observations better than when using only the rain gauge data. However, when using the unadjusted CML QPEs (method i), certain CMLs provide rainfall estimates which capture also the first runoff peak, which is not present at all in the case of the rain gauge data. However, even if the hydrograph timing looks reasonable, the unadjusted CML data often lead to highly overestimated discharges. The presented hydrographs exemplify well main features of different rainfall inputs affecting the overall results introduced further in the text, while suggesting that CML QPEs can provide reliable information about rainfall-runoff dynamics, but also emphasizing that the bias common in these data is a major problem that has to be dealt with carefully.

Model performance summarized for all relevant rainfall-runoff events

We hereby present the model performance summarized for the 59 rainfall-runoff events in the form of boxplots, where each boxplot belongs to one modelling scenario. We do this for the three metrics used to quantify the rainfall-runoff model performance.

Firstly, the model performance in terms of the dV and NSE metrics is depicted in Fig. 5. The results are considerably unalike for the two methods of deriving CML QPEs. For the unadjusted QPEs (Fig. 5, left), higher dV values tend to be associated with shorter CMLs. Such positive bias linked to the high sensitivity of short CML to wet antenna attenuation has been already observed in the past (e.g. Fencl et al., 2018). Furthermore, the variability of the dV values is smaller for long CMLs.

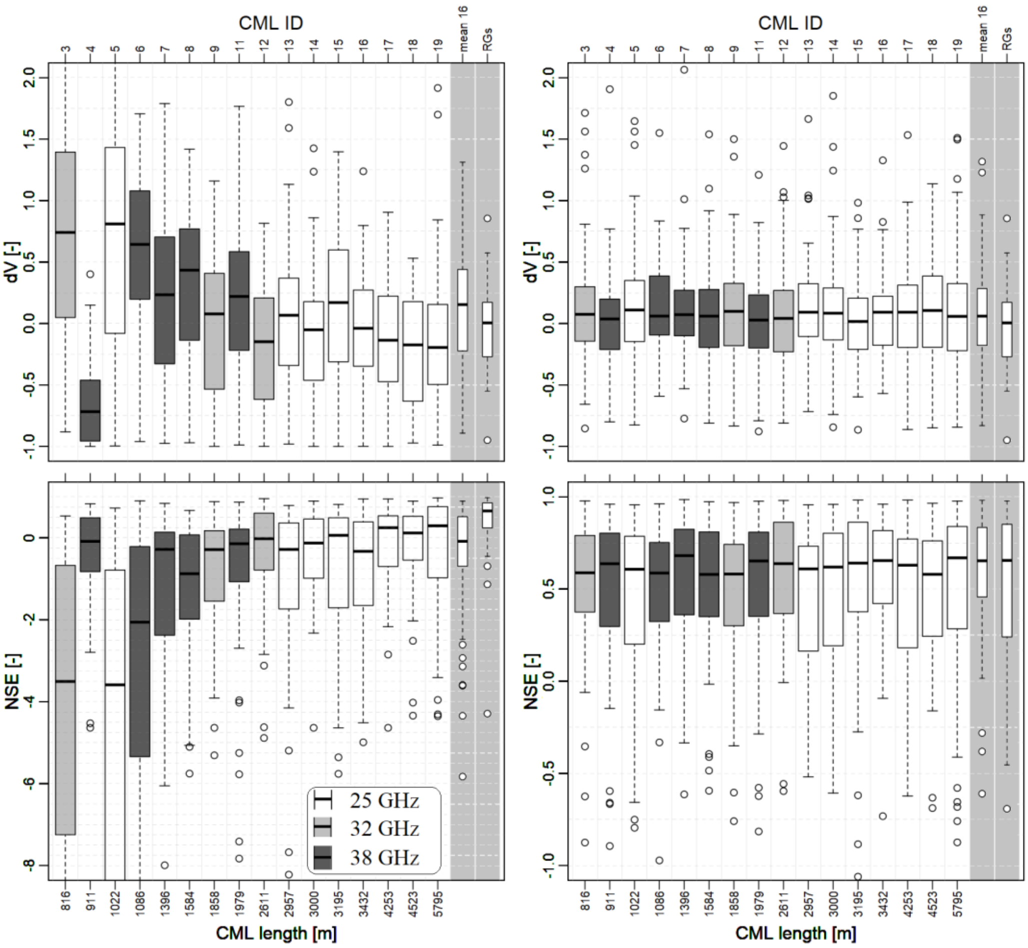

Fig. 5: Boxplots of dV (top row) and NSE (bottom row) performance metrics, summarized for all available rainfall-runoff events, obtained using the unadjusted CML QPEs (method I, left) and the CML QPEs adjusted to rain gauges (method ii, right). Note the different y-axes for the NSE.

However, the CML #4 is a distinctive exception to the observations formulated above. Although very short, this CML leads to substantially underestimated runoff volumes. However, additional analysis shows that there are unusually low values of attenuation observed on one of the two channels of this CML. Since we use the mean of the observed attenuation of the two channels to estimate the rainfall intensity, the intensities derived from this CML, and consequently also the simulated runoffs, are systematically underestimated.

In terms of NSE metric, the unadjusted CML QPEs (Fig. 5, bottom left) do not outperform the rain gauge data. For individual links, better NSE values (higher median, lower variability) are in general obtained for longer CMLs. However, as shown e.g. by the CML #4, this is not a universal rule. This, actually, confirms the crucial effect of the bias in CML QPEs on rainfall-runoff predictions, since, when we compare the dV and NSE metrics (Fig. 5, left), we see that the worst NSE values are connected to links leading to notably overestimated (30% to 100% in median) runoff volumes. The mean over all available CMLs provides relatively good results, very similar to (but not better than) the best performing individual CMLs.

The performance metrics for the adjusted CML QPEs (Fig. 5, right) are relatively alike, both in the median and variability, for all rainfall data sets we examine. There are no clear trends associated to the CML path length. The dV values for all CMLs, and also the mean over all CMLs, are similar to, but not better than the values obtained using the rain gauge data alone. These results show that adjusting CML QPEs to rain gauge data effectively minimizes the bias in the CML QPEs. Therefore, NSE values for the adjusted CML QPEs are notably higher than the values obtained using the unadjusted CML data. The results are in general very similar to those for the rain gauges, i.e. with the median roughly between 0.5 and 0.8, and with the interquartile range between 0.4 and 0.7. Most of the individual CMLs (including also short ones), and the mean over all CMLs as well, lead to less variable NSE values than the rain gauges. However, no CML QPEs lead to decisively higher median NSE values.

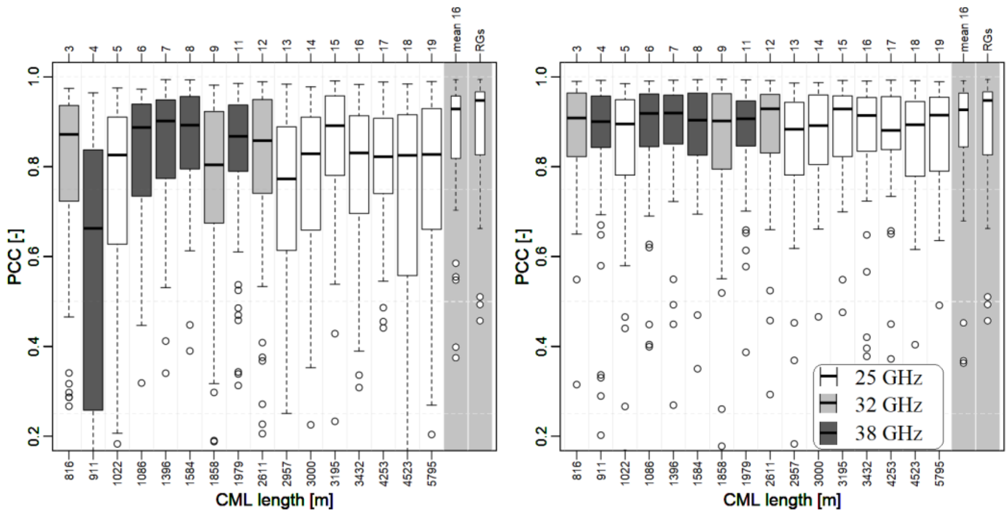

Fig. 6: Boxplots of PCC values, summarized for all available rainfall-runoff events, obtained using the unadjusted CML QPEs (method I, left) and the CML QPEs adjusted to rain gauges (method ii, right).

The model performance in terms of PCC (Fig. 6), which is insensitive to linear bias, in contrast to dV or NSE, does not show clear dependence on CML lengths. However, for the unadjusted QPEs (Fig. 6, left), it seems that, apart from the exceptional CML #4, better values are reached using

CMLs operating at the frequency of 38 GHz. Very low and variable PCC values are associated to the CML #4, which systematically underestimates runoff volumes (due to negative bias in the QPEs). Interestingly, the best performing CML QPEs, with performance similar to the rain gauges, are those derived from the mean of all available links. Adjusting to rain gauges (Fig. 6, right) considerably levels out the differences among the respective rainfall data sets. In general, it improves the results for the CML QPEs, mainly their variability, but the values obtained are not higher in median than for the rain gauges used alone. The performance of the mean over all available CMLs is rather mediocre in comparison to the QPEs from individual CMLs in this case.

Model performance and rainfall intensity

We analyze as well the relation between the model performance obtained using the CML QPEs and rainfall intensities. For these purposes, we classify roughly 1/3 of the studied events as heavy rainfalls (max. 10-min rainfall intensity > 12 mm/h). For more information see Tab. 3. Rainfall data obtained as the mean of the three local rain gauges (the same as used for the model calibration) is used for this classification.

	Light	Moderate	Heavy
Defining $R_{max,10}$ [mm/h]	$x \leq 5$	$5 < x < 12$	$12 \leq x$
Number of events	23	22	22

Tab. 3: Categorization of rainfalls. The defining maximal 10-min rainfall intensity $R_{max,10}$ as measured by the three rain gauges temporarily installed in the catchment

We observe no substantial differences in model performance in terms of the dV and NSE metrics for rainfalls events with various maximal intensities. However, as shown in Fig. 7, model performance reached using the CML QPEs in terms of the PCC metric is better for events with higher maximal 10-min intensities. This observation is valid for all QPEs derived from individual CMLs, as well as for their mean

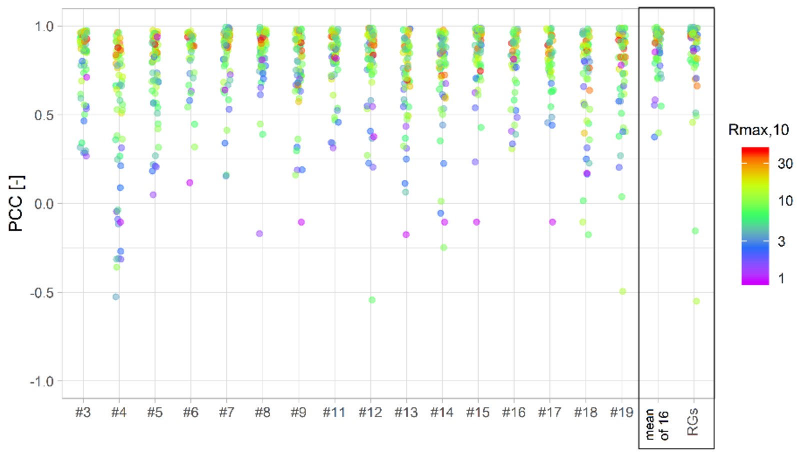

Fig. 7: Jitter-plots of the PCC metric reached using the unadjusted CML QPEs and the rain gauge data with color-coded max. 10-min rainfall intensities ($R_{max,10}$) of the individual events.

Interestingly, we observe the tendency depicted in the Fig. 7 only for unadjusted CML QPEs, as can be seen in Fig. 8, where the mean of QPEs from all available CMLs is analyzed more closely. This figure shows also that, for events with relatively high maximal 10-min rainfall intensity, the mean of CML QPEs in general leads to better PCC values than observations from the rain gauges

(Fig. 8, left) and also than CML QPEs adjusted to the rain gauges (Fig. 8, right). When comparing the adjusted CML QPEs and the rain gauge data (Fig. 8, middle), there is no clear difference between PCC values obtained using these data sets. This suggests that we can obtain very interesting information about dynamics of heavy events from unadjusted CML QPEs, but this information is not present in the adjusted CML QPEs.

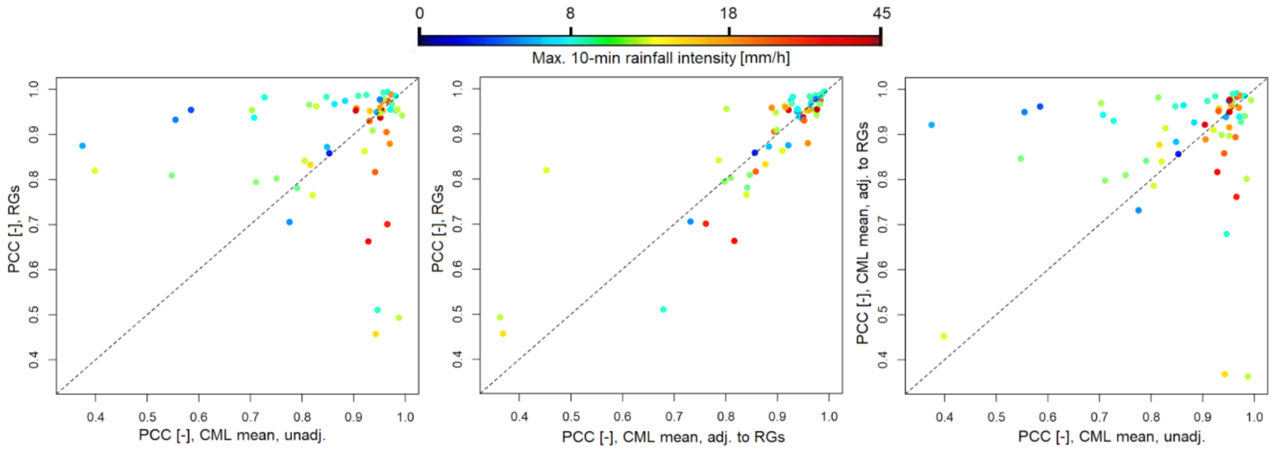

Fig. 8: Scatterplots of PCC for 3 rainfall data sets with color-coded max. 10-min rainfall intensities of the individual events. Left: The mean over unadjusted CML QPEs (x axis) and the rain gauges (y axis). Middle: The mean over CML QPEs adjusted to the rain gauges (x axis) and the rain gauges (y axis). Right: The mean over unadjusted CML QPEs (x axis) and the mean over CML QPEs adjusted to the rain gauges (y axis).

We hereby analyze more closely only the events classified as heavy rainfalls. Rainfall-runoff model performance as quantified by the dV and NSE metrics, summarized only for these heavy rainfalls, is depicted in Fig. 9 General tendencies are similar as when summarizing for all available events. For the unadjusted CML QPEs (Fig. 9, left), there still is a considerable dependency between these performance metrics and CML path length. However, the best NSE values are clearly associated with links which tend to underestimate the total discharged volumes, i.e. CMLs #4 and #19. The mean over QPEs from all individual CMLs still performs relatively well.

Similarly as when summarized for all available events, the CML QPEs are substantially less biased when adjusted to RGs (Fig. 9, top right). The results are relatively similar for all examined rainfall data sets. Nevertheless, this similarity is not so pronounced as when evaluating all events together. Especially the variability among the events is not dramatically reduced by the adjusting. The medians are relatively close to 0 in most of the cases and they are not significantly linked to the CML path lengths. The best dV values, predominantly in terms of variability, are not reached using data from the rain gauges, but using the mean over all individual CML QPEs, and QPEs from CMLs of moderate lengths working at high frequencies. NSE values for the adjusted CML QPEs (Fig. 9, bottom right) vary much less among various CMLs than for the unadjusted QPEs. The results are in general very similar to those for the rain gauges. Most of the individual CMLs (including also short ones) lead to less variable NSE values than the rain gauges. Interestingly, mean of the QPEs from all available CMLs performs as well as the best individual CML.

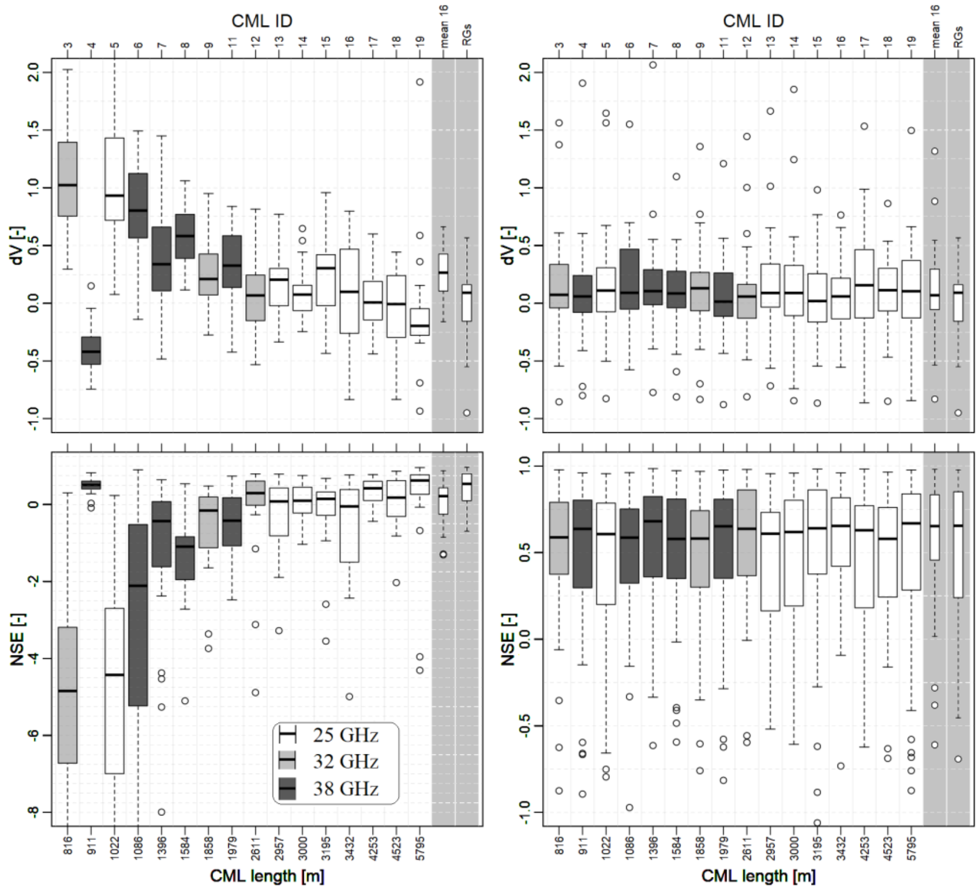

Fig. 9: Boxplots of dV (top row) and NSE (bottom row) performance metrics, summarized only for heavy rainfalls, obtained using the unadjusted CML QPEs (method I, left) and the CML QPEs adjusted to rain gauges (method ii, right). Note the different y-axes for the NSE.

As already shown before, the performance in terms of PCC is rather different than when summarized for all rainfall-runoff events. Most notably, the unadjusted CML QPEs (Fig. 10, left) lead now to higher PCC values (medians between 0.85 and 0.95). The mean over all CMLs leads to the best PCC values. For the individual CML QPEs, the best results are reached using relatively short CMLs located in the western part of the catchment which operate at high frequencies (#6, #7, #8). Individual links differ especially in the variability of the PCC values. The high variability is connected to longer CMLs reaching eastwards out of the catchment (#9, #13, #14, #17 and #18) and to those which tend to underestimate runoff volumes (#4 and #19).

For the CML QPEs adjusted to the rain gauges (Fig. 10, right), the PCC values are in median, and predominantly also in variability, similar to the values obtained when using only the rain gauge data. When compared to the unadjusted QPEs, the short CMLs (and the mean over all CMLs) lead in general to worse results, and the long links to better ones.

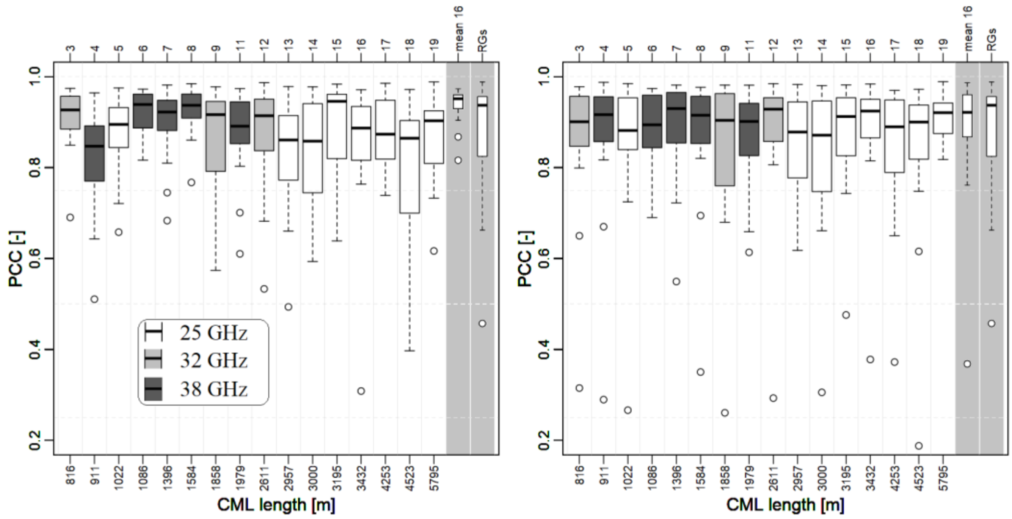

Fig. 10: Boxplots of PCC values, summarized only for heavy events, obtained using the unadjusted CML QPEs (method I, left) and the CML QPEs adjusted to rain gauges (method ii, right).

Discussion

In this study, we evaluate the suitability of QPEs from CMLs for urban drainage modelling, with a special focus on known CML characteristics influencing their sensitivity to rainfall. We do this by comparing simulated runoffs (obtained using the investigated data) with runoffs observed in the drainage system of the studied catchment.

In a study devoted to developing a framework for accounting for uncertainties in urban drainage models (Deletic et al., 2012), the following key uncertainty sources were identified: i) model input (measured input data and parameters) uncertainties; (ii) calibration (calibration data measuring, availability, and choices; calibration algorithms and objective functions used in the calibration process) uncertainties; (iii) model structure (conceptualization errors, equations and numerical methods).

As discussed earlier, in order to obtain unbiased QPEs from CMLs, the raindrop-induced attenuation has to be separated from other components of the total (observed) radio wave attenuation. The greatest challenge is to reliably estimate the so-called wet antenna attenuation (WAA), as it is a complex process highly dependent on site-specific conditions and characteristics of each single CML unit (e.g. antenna radome diameter, age, or coating). Furthermore, current methods for WAA estimation have been typically derived from specialized experiments, and thus, they are often unable to take into account all the case-specific factors. Therefore, incorrect WAA estimation is a common source of errors in CML QPEs. When compared to the raindrop-induced attenuation, WAA is relatively large especially for short CMLs (path lengths < 2000 m). Therefore, the errors due to incorrect WAA estimation are likely to affect most gravely QPEs from these short CMLs. This has been largely confirmed by our results (for CML QPEs not adjusted to rain gauge data), indicating that the WAA estimation process has to be improved in order to obtain unbiased QPEs, especially from short CMLs.

Apart from the input rainfall data, which are the main object of interest in our study, the results are affected by uncertainties associated with the rainfall-runoff model, especially its calibration. As mentioned earlier, the model was calibrated before the start of this study using point information from rain gauges installed directly in the catchment. The data set used for the model calibration contained a relatively small number of events, thus, we performed model validation (details provided earlier) using rainfall measurements from the same devices but covering the time period as in the main part of the study, i.e. three summer seasons. This validation shows that the model was calibrated satisfactorily for usage with the data from the local rain gauges. However, when simulating rainfall-runoff processes in the studied catchment using various rainfall data sets, the model has not been recalibrated to the respective new rainfall data. Therefore, it might be argued that the potentially unsatisfying model performance obtained using the new data is only due to the lack of calibration to these data, and that it might have been better if the model was calibrated properly. This is valid especially for CML QPEs, since they contain path-integrated rainfall information the nature of which is notably different than in the case of traditional rain gauges.

Discharge observations represent additional source of uncertainty, not relevant only during calibration, but also when evaluating the simulations, since these measurements are the reference used to calculate the model performance metrics. We estimated the standard uncertainty and the expanded uncertainty of the measured flow rate. These estimated uncertainties reach considerable values, especially for low discharges (±31.0% for the Q = 0.091 $m^3.s^{-1}$). Nevertheless, such levels could be expected, since we used a relatively high estimate of the standard uncertainty of measured flow depth, which had been reported appropriate during events whereby flow unsteadiness and turbulence levels are considerable (Muste et al., 2012).

It is a common approach (e.g. Krajewski et al., 2010; Emmanuel et al., 2012; Fencl et al., 2017) to evaluate and benchmark rainfall data sets by a direct comparison with a referential (e.g. best-case scenario) data set. However, especially for applications where spatiotemporal resolution plays a crucial role, such as urban drainage modelling, the limited representativeness of the referential rainfall data set is a considerable issue, especially if radar data are being compared with point rain gauge observations (Gires et al., 2014). If, as reference, we use even high-quality precipitation measurements, e.g. from a relatively dense network of rain gauges, the information about precipitation included in such data can differ substantially from the true incident rainfall over a given area. Even if we are not interested in areal, but only path-integrated rainfall, as in our case, a large number of rain gauges would be necessary to obtain the rainfall information in desired resolution. Furthermore, if we were to evaluate a data set which happens to better describe the ground-truth precipitation than the referential rainfall data, the superiority of the new data could not be confirmed using this approach.

However, if rainfall data sets are evaluated primarily for purposes of urban drainage modelling, as in our case, it is common to assess the model performance while using the examined rainfall data as model inputs. This is done also in the study of Ochoa-Rodriguez et al. (2015) on the impact of spatial and temporal resolution of rainfall inputs on urban hydrodynamic modelling. However, in that study, modelling outputs obtained using various rainfall data sets were evaluated using, as reference, modelling outputs associated to the finest resolution rainfall estimates. Nevertheless, since discharges in traditional urban drainage systems typically closely reflect transformed rainfall, aggregated for a whole given catchment, it seems intuitive to use discharge measurements when evaluating the performance of urban drainage modelling with the given rainfall data, as done e.g. by Goormans and Willems (2013), Dotto et al. (2014), or Wang et al. (2015).

Conclusions

In this paper, we evaluate the suitability of quantitative precipitation estimates (QPEs) from commercial microwave links (CMLs) for urban drainage modelling. Using as case study a dataset from three summer seasons collected in a small (1.3 km^2) urban catchment in Prague-Letňany, we compare runoffs observed in the catchment with runoffs simulated using the various investigated rainfall data, especially QPEs derived from individual CMLs. This enables us to investigate how the position and characteristics (such as frequency or length scale over which they integrate rainfall information) of the individual CMLs influence their suitability for rainfall-runoff modeling.

The results show that:

- The sensitivity of CMLs to rainfall, which is given by their frequency, polarization, and length, is the most influential factor affecting accuracy of CML QPEs, especially their systematic under- or over estimation. This bias propagates into rainfall-runoff predictions and affects also other volumetric statistics such as Nash-Sutcliffe Efficiency. The bias is largest for the shortest CMLs. QPEs from all CMLs perform in terms of volumetric statistics worse than remote (approx. 2.5 km far) rain gauges. The position of CMLs has minor effect on volumetric statistics, and this holds even during heavy rainfalls with high space-time variability and even for the longest CMLs with most of the path reaching out of the catchment borders.
- The bias in CML QPEs is variable within the events and is, in general, more pronounced for light rainfalls. The ability of these CML data to provide reliable flow estimates during these light events is predominantly low.
- The position of CMLs with respect to the catchment affects their ability to capture rainfall-runoff dynamics, e.g. the beginning of a runoff event, timing of the hydrograph rising limb, runoff peak, and recession limb. The effect of CML position is especially pronounced during heavy rainfalls, when shorter CMLs with paths within or close to the catchment borders reproduce runoff dynamics better than longer CMLs reaching outside of the catchment.
- The best performance in terms of capturing runoff dynamics is obtained when rainfall observations of all the CMLs are averaged. Especially promising results are obtained during heavy rainfall events, for which correlation coefficient varies between 0.82 and 0.97 with median 0.95. These are substantially larger correlations than those obtained when simulating runoff using remote rain gauges. The CML mean rainfall performs relatively well also with respect to volumetric statistics, nevertheless, the best performing (long) CMLs, as well as remote rain gauges, outperform the CML mean both in terms of systematic errors and Nash-Sutcliffe Efficiency.
- The adjusting of CML QPEs to remote rain gauges substantially reduces the bias. Moreover, the mean over all adjusted CML QPEs slightly outperforms the remote rain gauges used alone in terms of Nash-Sutcliffe Efficiency. However, the adjusting worsens the ability of CML QPEs to reproduce runoff dynamics during heavy rainfalls.

This study shows that QPEs derived from CMLs can improve rainfall-runoff simulations, nevertheless, they are more suitable for applications where reproducing of runoff dynamics is more important than correct estimation of runoff volume. Reduction of the systematic errors in these rainfall data remains the major challenge compromising their usage for applications where runoff volume is essential (e.g. modelling of water balance, or design of large retention tanks). However, CML networks are available worldwide, and thus, they represent a potentially very promising source of rainfall information, especially for sparsely gauged or completely ungauged regions. When traditional rainfall observations are not available, mean areal rainfall obtained from all CMLs covering a given catchment represents the most robust input for rainfall-runoff modeling.

Our further research concentrates on the reduction of systematic errors in CML QPEs, and on the rainfall retrieval from the new generation of E-band CMLs. These CMLs operate at frequencies between 71 and 86 GHz, what makes them about three times more sensitive to attenuation due to raindrops than older (20 - 40 GHz) CML devices, and thus, they could be less prone to systematic errors caused by antenna wetting and by quantization of recorded attenuation levels.

Acknowledgment

This study was supported by the project no. 17-16389S of the Czech Science Foundation and by the project of the Czech Technical University in Prague no. SGS18/053/OHK1/1T/11.

Bibliography

Anagnostou, E.N., Krajewski, W.F., Smith, J., 1999. Uncertainty Quantification of Mean-Areal Radar-Rainfall Estimates. Journal of Atmospheric and Oceanic Technology 16, 206–215. https://doi.org/10.1175/1520-0426(1999)016<0206:UQOMAR>2.0.CO;2

Atlas, D., Ulbrich, C.W., 1977. Path- and Area-Integrated Rainfall Measurement by Microwave Attenuation in the 1–3 cm Band. J. Appl. Meteorol. 16, 1322–1331. https://doi.org/10.1175/1520-0450(1977)016<1322:PAAIRM>2.0.CO;2

Berne, A., Delrieu, G., Creutin, J.-D., Obled, C., 2004. Temporal and spatial resolution of rainfall measurements required for urban hydrology. J. Hydrol. 299, 166–179. https://doi.org/10.1016/j.jhydrol.2004.08.002

Borup, M., Grum, M., Linde, J.J., Mikkelsen, P.S., 2016. Dynamic gauge adjustment of high-resolution X-band radar data for convective rain storms: Model-based evaluation against measured combined sewer overflow. J. Hydrol. 539, 687–699. https://doi.org/10.1016/j.jhydrol.2016.05.002

Chwala, C., Keis, F., Kunstmann, H., 2016. Real-time data acquisition of commercial microwave link networks for hydrometeorological applications. Atmospheric Meas. Tech. 9, 991–999. https://doi.org/10.5194/amt-9-991-2016

D’Amico, M., Manzoni, A., Solazzi, G.L., 2016. Use of Operational Microwave Link Measurements for the Tomographic Reconstruction of 2-D Maps of Accumulated Rainfall. IEEE Geoscience and Remote Sensing Letters 13, 1827–1831. https://doi.org/10.1109/LGRS.2016.2614326

de Vos, L., Leijnse, H., Overeem, A., Uijlenhoet, R., 2017. The potential of urban rainfall monitoring with crowdsourced automatic weather stations in Amsterdam. Hydrol. Earth Syst. Sci. 21, 765–777. https://doi.org/10.5194/hess-21-765-2017

Deletic, A., Dotto, C.B.S., McCarthy, D.T., Kleidorfer, M., Freni, G., Mannina, G., Uhl, M., Henrichs, M., Fletcher, T.D., Rauch, W., Bertrand-Krajewski, J.L., Tait, S., 2012. Assessing uncertainties in urban drainage models. Phys. Chem. Earth Parts ABC 42–44, 3–10. https://doi.org/10.1016/j.pce.2011.04.007

Dotto, C.B.S., Kleidorfer, M., Deletic, A., Rauch, W., McCarthy, D.T., 2014. Impacts of measured data uncertainty on urban stormwater models. J. Hydrol. 508, 28–42. https://doi.org/10.1016/j.jhydrol.2013.10.025

Einfalt, T., Arnbjerg-Nielsen, K., Golz, C., Jensen, N.-E., Quirmbach, M., Vaes, G., Vieux, B., 2004. Towards a roadmap for use of radar rainfall data in urban drainage. Journal of Hydrology 299, 186–202. https://doi.org/10.1016/j.jhydrol.2004.08.004

Ellis, J.B., 2000. Risk assessment approaches for ecosystem responses to transient pollution events in urban receiving waters. Chemosphere 41, 85–91. https://doi.org/10.1016/S0045-6535(99)00393-8

Emmanuel, I., Andrieu, H., Leblois, E., Flahaut, B., 2012. Temporal and spatial variability of rainfall at the urban hydrological scale. J. Hydrol. 430–431, 162–172. https://doi.org/10.1016/j.jhydrol.2012.02.013

Ericsson, 2016. Ericsson Microwave Outlook [WWW Document]. URL https://www.ericsson.com/assets/local/microwave-outlook/documents/ericsson-microwave-outlook-report-2016.pdf (accessed 7.15.17).

Fencl, M., Dohnal, M., Rieckermann, J., Bareš, V., 2017. Gauge-adjusted rainfall estimates from commercial microwave links. Hydrol. Earth Syst. Sci. 21, 617–634. https://doi.org/10.5194/hess-21-617-2017

Fencl, M., Rieckermann, J., Sýkora, P., Stránský, D., Bareš, V., 2015. Commercial microwave links instead of rain gauges: fiction or reality? Water Sci. Technol. 71, 31–37. https://doi.org/10.2166/wst.2014.466

Fencl, M., Valtr, P., Kvičera, M., Bareš, V., 2018. Quantifying Wet Antenna Attenuation in 38-GHz Commercial Microwave Links of Cellular Backhaul. IEEE Geoscience and Remote Sensing Letters 1–5. https://doi.org/10.1109/LGRS.2018.2876696

Fenicia, F., Pfister, L., Kavetski, D., Matgen, P., Iffly, J.-F., Hoffmann, L., Uijlenhoet, R., 2012. Microwave links for rainfall estimation in an urban environment: Insights from an experimental setup in Luxembourg-City. J. Hydrol. 464–465, 69–78. https://doi.org/10.1016/j.jhydrol.2012.06.047

Gharesifard, M., Wehn, U., van der Zaag, P., 2017. Towards benchmarking citizen observatories: Features and functioning of online amateur weather networks. J. Environ. Manage. 193, 381–393. https://doi.org/10.1016/j.jenvman.2017.02.003

Gires, A., Onof, C., Maksimovic, C., Schertzer, D., Tchiguirinskaia, I., Simoes, N., 2012. Quantifying the impact of small scale unmeasured rainfall variability on urban runoff through multifractal downscaling: A case study. J. Hydrol. 442–443, 117–128. https://doi.org/10.1016/j.jhydrol.2012.04.005

Gires, A., Tchiguirinskaia, I., Schertzer, D., Schellart, A., Berne, A., Lovejoy, S., 2014. Influence of small scale rainfall variability on standard comparison tools between radar and rain gauge data. Atmospheric Res. 138, 125–138. https://doi.org/10.1016/j.atmosres.2013.11.008

Giuli, D., Toccafondi, A., Gentili, G.B., Freni, A., 1991. Tomographic Reconstruction of Rainfall Fields through Microwave Attenuation Measurements. J. Appl. Meteorol. 30, 1323–1340. https://doi.org/10.1175/1520-0450(1991)030<1323:TRORFT>2.0.CO;2

Goormans, T., Willems, P., 2013. Using Local Weather Radar Data for Sewer System Modeling: Case Study in Flanders, Belgium. J. Hydrol. Eng. 18, 269–278. https://doi.org/10.1061/(ASCE)HE.1943-5584.0000589

Gosset, M., Kunstmann, H., Zougmore, F., Cazenave, F., Leijnse, H., Uijlenhoet, R., Chwala, C., Keis, F., Doumounia, A., Boubacar, B., Kacou, M., Alpert, P., Messer, H., Rieckermann, J., Hoedjes, J., 2016. Improving Rainfall Measurement in Gauge Poor Regions Thanks to

Mobile Telecommunication Networks. Bull. Am. Meteorol. Soc. 97, ES49–ES51. https://doi.org/10.1175/BAMS-D-15-00164.1

Harrison, D.L., Scovell, R.W., Kitchen, M., 2009. High-resolution precipitation estimates for hydrological uses. Proc. Inst. Civ. Eng. - Water Manag. 162, 125–135. https://doi.org/10.1680/wama.2009.162.2.125

Heistermann, M., Jacobi, S., Pfaff, T., 2013. Technical Note: An open source library for processing weather radar data (wradlib). Hydrol. Earth Syst. Sci. 17, 863–871. https://doi.org/10.5194/hess-17-863-2013

Humphrey, M.D., Istok, J.D., Lee, J.Y., Hevesi, J.A., Flint, A.L., 1997. A New Method for Automated Dynamic Calibration of Tipping-Bucket Rain Gauges. J. Atmospheric Ocean. Technol. 14, 1513–1519. https://doi.org/10.1175/1520-0426(1997)014<1513:ANMFAD>2.0.CO;2

International Bureau of Weights and Measures, International Organization for Standardization (Eds.), 1993. Guide to the expression of uncertainty in measurement, 1st ed. International Organization for Standardization, Genève, Switzerland.

ITU Radiocommunication Sector, 2005. Recommendation 838-3: Specific attenuation model for rain for use in prediction methods. http://www.itu.int/dms_pubrec/itu-r/rec/p/R-REC-P.838-3-200503-I!!PDF-E.pdf (last access: 23 Oct. 2018).

Kharadly, M.M.Z., Ross, R., 2001. Effect of wet antenna attenuation on propagation data statistics. IEEE Transactions on Antennas and Propagation 49, 1183–1191. https://doi.org/10.1109/8.943313

Kidd, C., Huffman, G., 2011. Global precipitation measurement: Global precipitation measurement. Meteorol. Appl. 18, 334–353. https://doi.org/10.1002/met.284

Krajewski, W.F., Villarini, G., Smith, J.A., 2010. Radar-Rainfall Uncertainties: Where are We after Thirty Years of Effort? Bull. Am. Meteorol. Soc. 91, 87–94. https://doi.org/10.1175/2009BAMS2747.1

Leijnse, H., Uijlenhoet, R., Stricker, J.N.M., 2008. Microwave link rainfall estimation: Effects of link length and frequency, temporal sampling, power resolution, and wet antenna attenuation. Adv. Water Resour. 31, 1481–1493. https://doi.org/10.1016/j.advwatres.2008.03.004

Leijnse, H., Uijlenhoet, R., Stricker, J.N.M., 2007. Rainfall measurement using radio links from cellular communication networks: RAPID COMMUNICATION. Water Resour. Res. 43. https://doi.org/10.1029/2006WR005631

Leth, T.C. van, Overeem, A., Leijnse, H., Uijlenhoet, R., 2018. A measurement campaign to assess sources of error in microwave link rainfall estimation. Atmospheric Meas. Tech. 11, 4645–4669. https://doi.org/10.5194/amt-11-4645-2018

Lorenz, C., Kunstmann, H., 2012. The Hydrological Cycle in Three State-of-the-Art Reanalyses: Intercomparison and Performance Analysis. J. Hydrometeorol. 13, 1397–1420. https://doi.org/10.1175/JHM-D-11-088.1

Messer, H., Zinevich, A., Alpert, P., 2006. Environmental Monitoring by Wireless Communication Networks. Science 312, 713–713. https://doi.org/10.1126/science.1120034

Montesarchio, V., Lombardo, F., Napolitano, F., 2009. Rainfall thresholds and flood warning: an operative case study. Natural Hazards and Earth System Sciences 9, 135–144. https://doi.org/10.5194/nhess-9-135-2009

Ochoa-Rodriguez, S., Wang, L.-P., Gires, A., Pina, R.D., Reinoso-Rondinel, R., Bruni, G., Ichiba, A., Gaitan, S., Cristiano, E., van Assel, J., Kroll, S., Murlà-Tuyls, D., Tisserand, B., Schertzer, D., Tchiguirinskaia, I., Onof, C., Willems, P., ten Veldhuis, M.-C., 2015. Impact of spatial and temporal resolution of rainfall inputs on urban hydrodynamic modelling outputs:

A multi-catchment investigation. J. Hydrol. 531, 389–407. https://doi.org/10.1016/j.jhydrol.2015.05.035
Olsen, R., Rogers, D., Hodge, D., 1978. The aRb relation in the calculation of rain attenuation. IEEE Trans. Antennas Propag. 26, 318–329. https://doi.org/10.1109/TAP.1978.1141845
Overeem, A., Leijnse, H., Uijlenhoet, R., 2011. Measuring urban rainfall using microwave links from commercial cellular communication networks: MEASURING URBAN RAINFALL USING MICROWAVE LINKS. Water Resour. Res. 47. https://doi.org/10.1029/2010WR010350
Rauch, W., Harremoës, P., 1996. The importance of the treatment plant performance during rain to acute water pollution. Water Science and Technology 34. https://doi.org/10.1016/0273-1223(96)00549-5
Schilling, W., 1991. Rainfall data for urban hydrology: what do we need? Atmospheric Res. 27, 5–21. https://doi.org/10.1016/0169-8095(91)90003-F
Schleiss, M., Rieckermann, J., Berne, A., 2013. Quantification and Modeling of Wet-Antenna Attenuation for Commercial Microwave Links. IEEE Geoscience and Remote Sensing Letters 10, 1195–1199. https://doi.org/10.1109/LGRS.2012.2236074
Schütze, M., Campisano, A., Colas, H., Schilling, W., Vanrolleghem, P.A., 2004. Real time control of urban wastewater systems - Where do we stand today? J. Hydrol. 299, 335–348. https://doi.org/10.1016/j.jhydrol.2004.08.010
Smiatek, G., Keis, F., Chwala, C., Fersch, B., Kunstmann, H., 2017. Potential of commercial microwave link network derived rainfall for river runoff simulations. Environ. Res. Lett. 12, 034026. https://doi.org/10.1088/1748-9326/aa5f46
Spekkers, M.H., Kok, M., Clemens, F.H.L.R., ten Veldhuis, J.A.E., 2013. A statistical analysis of insurance damage claims related to rainfall extremes. Hydrology and Earth System Sciences 17, 913–922. https://doi.org/10.5194/hess-17-913-2013
Stránský, D., Fencl, M., Bareš, V., 2018. Runoff prediction using rainfall data from microwave links: Tabor case study. Water Sci. Technol. 2017, 351–359. https://doi.org/10.2166/wst.2018.149
Swan, M., 2012. Sensor Mania! The Internet of Things, Wearable Computing, Objective Metrics, and the Quantified Self 2.0. J. Sens. Actuator Netw. 1, 217–253. https://doi.org/10.3390/jsan1030217
Tauro, F., Selker, J., van de Giesen, N., Abrate, T., Uijlenhoet, R., Porfiri, M., Manfreda, S., Caylor, K., Moramarco, T., Benveniste, J., Ciraolo, G., Estes, L., Domeneghetti, A., Perks, M.T., Corbari, C., Rabiei, E., Ravazzani, G., Bogena, H., Harfouche, A., Brocca, L., Maltese, A., Wickert, A., Tarpanelli, A., Good, S., Lopez Alcala, J.M., Petroselli, A., Cudennec, C., Blume, T., Hut, R., Grimaldi, S., 2018. Measurements and Observations in the XXI century (MOXXI): innovation and multi-disciplinarity to sense the hydrological cycle. Hydrol. Sci. J. 63, 169–196. https://doi.org/10.1080/02626667.2017.1420191
ten Veldhuis, J.A.E., Clemens, F.H.L.R., Sterk, G., Berends, B.R., 2010. Microbial risks associated with exposure to pathogens in contaminated urban flood water. Water Research 44, 2910–2918. https://doi.org/10.1016/j.watres.2010.02.009
Tsihrintzis, V.A., Hamid, R., 1997. Modeling and Management of Urban Stormwater Runoff Quality: A Review. Water Resour. Manag. 11, 136–164. https://doi.org/10.1023/A:1007903817943
van der Pol, T.D., van Ierland, E.C., Gabbert, S., Weikard, H.-P., Hendrix, E.M.T., 2015. Impacts of rainfall variability and expected rainfall changes on cost-effective adaptation of water systems to climate change. Journal of Environmental Management 154, 40–47. https://doi.org/10.1016/j.jenvman.2015.02.016

Vezzaro, L., Grum, M., 2014. A generalised Dynamic Overflow Risk Assessment (DORA) for Real Time Control of urban drainage systems. Journal of Hydrology 515, 292–303. https://doi.org/10.1016/j.jhydrol.2014.05.019

Wang, L.-P., Ochoa-Rodríguez, S., Onof, C., Willems, P., 2015. Singularity-sensitive gauge-based radar rainfall adjustment methods for urban hydrological applications. Hydrol Earth Syst Sci 19, 4001–4021. https://doi.org/10.5194/hess-19-4001-2015

Wang, L.-P., Ochoa-Rodríguez, S., Simões, N.E., Onof, C., Maksimović, Č., 2013. Radar–raingauge data combination techniques: a revision and analysis of their suitability for urban hydrology. Water Sci. Technol. 68, 737–747. https://doi.org/10.2166/wst.2013.300

Willems, P., Arnbjerg-Nielsen, K., Olsson, J., Nguyen, V.T.V., 2012. Climate change impact assessment on urban rainfall extremes and urban drainage: Methods and shortcomings. Atmospheric Research 103, 106–118. https://doi.org/10.1016/j.atmosres.2011.04.003

Zevenbergen, C., Veerbeek, W., Gersonius, B., Van Herk, S., 2008. Challenges in urban flood management: travelling across spatial and temporal scales: Challenges in urban flood management. Journal of Flood Risk Management 1, 81–88. https://doi.org/10.1111/j.1753-318X.2008.00010.

Zinevich, A., Alpert, P., Messer, H., 2008. Estimation of rainfall fields using commercial microwave communication networks of variable density. Adv. Water Resour. 31, 1470–1480. https://doi.org/10.1016/j.advwatres.2008.03.003